Multilayer Analysis of Anisotropic Heat Flux in Vertical Cavity-Surface Emitting Lasers With Quarter-Wave Semiconducting Mirrors

Antonio A. Leal, Marek Osiński, *Senior Member, IEEE,* and Evandro Conforti, *Senior Member, IEEE*

***Abstract*—Monolithic arrays of vertical cavity-surface emitting lasers (VCSEL's) have the potential to be used in microwave systems based on opto-electronic technologies. However, the temperature has a strong influence over several characteristics of VCSEL's. Self heating may restrain the gain inside the device cavity and it is responsible for an increase in the laser threshold current as well as a decrease of its output power. In this paper, the thermal behavior of VCSEL's was evaluated by means of a procedure that takes into account the multilayer aspects of the heat-flux propagation. The method has the advantage of dealing with the heat propagation inside each layer of the periodic structures of the device. Thus, the different characteristics and influence of the materials employed in the chip manufacturing can be considered and the device temperature profile can be predicted. From the method assumptions and simulations, the thermal resistances of typical devices were calculated. The results were shown to be in good agreement with experimental values reported in the literature.**

***Index Terms*— Heat flux in quarter-wave semiconductor mirrors, thermal influence, vertical cavity-surface emitting laser.**

I. Introduction

VERTICAL cavity-surface emitting lasers (VCSEL's) [1] are promising devices for applications where the beams of an array of lasers must be coupled into an array of optical fibers, such as in optical interconnections. The array configuration could also be applied to microwave systems such as in phased-array antennas [2], [3], due to the possibility of obtaining true time delay network operation. In this latter case, a two-dimensional (2-D) array of VCSEL's could provide a source with several switched lasers whose beams are coupled into the fibers of appropriate lengths for the optical delay control. The optical coupling between the fibers and the lasers could be efficiently accomplished due to the nearly intrinsic circular emission profile of VCSEL's. In addition to that, the laser fabrication employs an entirely monolithic process, leading to efficiently packed 2-D arrays; the initial probe test can be performed before laser cleaving, longitudinal single-mode operation is ensured by the small distance between the mirrors of the VCSEL, and very fast optical pulses can be obtained [4].

Despite recent progresses, the continuous-wave (CW) operation of VCSEL's is still severely limited by thermal problems. The self-heating in VCSEL's is mainly due to the Joule effect between the quarter-wave mirrors as well as to the nonradiative recombination and the free carrier absorption in the active region. The active-region temperature increases as heat is generated inside the device and a negative impact over the threshold current density, the gain inside the quantum wells, and the wavelength shifts are observed [5]. Therefore, the understanding of the thermal effects in VCSEL's is important. Furthermore, a proper heat distribution can also lead to a device enhanced performance. An example of that is the superior beam spatial distribution of the VCSEL's caused by an intrinsic thermal lensing effect, when compared with conventional semiconductor lasers.

A complete analysis of the influence of heating over the electrical and optical characteristics of the VCSEL's would require the heat conduction equations to be solved simultaneously with the usual laser rate equations. This results in a high-order system of differential equations, and the complete analysis of thermal problems in VCSEL's can be very involved.

An alternative approach to deal with the thermal problem analysis is to use the concept of thermal resistance. Methods employing this simple concept are attractive as easy-to-measure quantities are employed and the calculation time is greatly reduced [6]. However, most of them do not furnish any information about temperature profile inside the laser. Moreover, as the complex device structure is substituted by a thermal equivalent single layer, all information about heat-flux propagation is lost.

In this paper, a method to evaluate the thermal resistance of a VCSEL, considering the heat spreading within the device layers and providing the laser temperature profile, is proposed. The heat flux is calculated by assuming the heat propagation through the easiest possible path (analogous to Fermats principle in optics). The anisotropic heat flux inside both the thin interfaces of quarter-wave mirrors and the separated confinement regions (SCH's) is also considered.

Manuscript received December 10, 1997; revised December 10, 1997. This work was supported in part by CPqD-Telebrás, PRONEX/MCT, CNPq, and FAPESP.

A. A. Leal is with the Faculty of Electrical and Computer Engineering, State University of Campinas, DMO/FEEC/Unicamp, CEP 13.083-970, Campinas-Sp, Brazil.

M. Osiński is with the Center of High Technology Materials, University of New Mexico, Albuquerque, NM 87131 USA.

E. Conforti is with the Faculty of Electrical and Computer Engineering, State University of Campinas, DMO/FEEC/Unicamp, Campinas-Sp, Brazil.

Publisher Item Identifier S 0018-9480(98)02035-3.

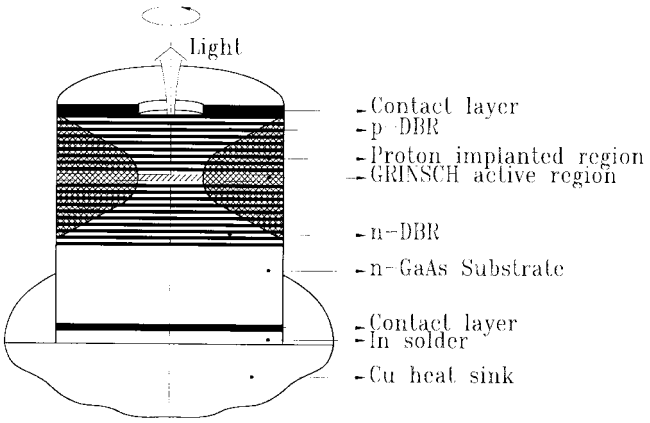

Fig. 1. Device schematic of a typical PITSEL.

II. Basic Theory

The thermal resistance of a VCSEL can be defined as follows [6]:

$$R_{\text{th}} \triangleq \frac{\Delta T_A}{P_{IV} - P_{hv}} \tag{1}$$

where ΔT_A is the active region temperature increase (kelvin); P_{IV} is the electric power supplied to the device (watt); and P_{hv} is the optical power (watt).

The device analyzed in this paper is a proton-implanted top-surface emitting laser (PITSEL) [7], as shown in Fig. 1. The active region is formed by a graded-index separate-confinement heterostructure (GRINSCH) with four 80-Å GaAs quantum wells. In each branch of the GRINSCH region, which is 1025-Å wide, the aluminum composition is linearly graded from the barrier composition (15%) to 55%. Different numbers for the n-distributed-Bragg-reflector (DBR) grating periods will be considered in the following analysis.

In CW operation, VCSEL's are likely to have high electrical series resistance, leading to considerable ohmic dissipation and, therefore, the output power limitation. The high electrical series resistance is mainly a result of carriers trying to overcome high potential barriers at the interfaces of the heterostructures of quarter-wave mirrors. It is known that graded composed interfaces offer a reduction in such potential barriers due to suppression of abrupt gaps in the energy band.

For ternary III–V compounds, the thermal conductivity (in watt per meter times kelvin) can be given by the following expression [8], where x is the molar fraction:

$$k(x) = (A + Bx - Cx^2)^{-1}. \tag{2}$$

In particular, for $Al_xGa_{1-x}As$ at room temperature, the parameters that appear in (2) are given by [9]: $A = 2.27\ 10^{-2}$ m· K/W, $B = 2.883\ 10^{-1}$ m· K/W, and $C = 3.00\ 10^{-1}$ m· K/W.

The anisotropic heat flux in graded composed layers is described by two components of thermal conductivity. We define an average radial thermal conductivity $k_{G,r}$ (in watt per meter times kelvin) as the parallel association of uniform layers with infinitesimal thickness [6], so that the following expression is valid:

$$k_{G,r} = \left(\int_0^{d_G} k(z)\, dz \right) \Big/ d_G \tag{3}$$

where: 1) d_G is the thickness of the graded layer and 2) z is the vertical coordinate.

Similarly, the average thermal conductivity for the vertical flux $k_{G,z}$ is defined as a series combination of uniform layers with infinitesimal thickness [6], resulting in the expression:

$$k_{G,z} = d_G / \int_0^{d_G} \frac{dz}{k(z)}. \tag{4}$$

According to (2)–(4), the thermal conduction inside graded layers is locally dependent on the position. The relation between the position coordinates and doping will be dictated by the grading profile. For the simple case of linear grading used in the device considered here, we can write

$$x(z) = x_H + (x_L - x_H)(z/d_G) \tag{5}$$

where x_L is the Al concentration (molar fraction) for the low refractive DBR layer, and x_H is Al concentration for the high refractive layer.

Equations (2), (3), and (5) lead to the following analytic expression for the radial thermal conductivity in linearly graded layers:

$$k_{G,r} = \frac{1}{E_G} \ln \left| \frac{2A + B(x_L + x_H) - 2Cx_Lx_H + E_G}{2A + B(x_L + x_H) - 2Cx_Lx_H - E_G} \right| \tag{6}$$

where

$$E_G = (x_L - x_H)(B^2 + 4AC)^{1/2}. \tag{7}$$

Similarly, the thermal conductivity of the vertical flux in linearly graded layers is given by

$$k_{G,z} = \frac{3}{A + \frac{1}{2}B(x_L + x_H) - C(x_L^2 + x_Lx_H + x_H^2)}. \tag{8}$$

In [6], we have demonstrated that for the calculation of the heat spreading inside the laser all the heat sources can be substituted by an equivalent source placed in the active region. This equivalent heat source is evenly distributed over the active area. Below the active region is a stack of cylinders formed by the VCSEL DBR layers. The heat spreading inside the layer j will only occupy a fraction D_{A_j} of the layer lateral dimension. By considering the anisotropic heat propagation in graded layers, the thermal conductivities for the vertical and the radial flux in layer j are given by k_{z_j} and k_{r_j}, respectively. The cumulative thickness d_{c_j} is defined as the distance from the active region to the end of layer j. The contribution of layer j to total thermal resistance is described in terms of the layer thickness d_j, the input heat-flux diameter for layer j, D_{Aj-1}, and the output heat-flux diameter for layer j, D_{Aj}, as follows [10]:

$$R_{\text{th}_j} = \frac{4dj}{\pi \cdot k_{z_j} \cdot D_{A_j}^2} + \frac{1}{2k_{r_j} \cdot D_{A_{j-1}}} \cdot \left(1 - \frac{D_{A_{j-1}}}{D_{A_j}} \right)^{3/2}. \tag{9}$$

The device thermal resistance $R_{\rm th}$ is obtained by summing up the elementary thermal resistance associated with all layers. The best thermal path is found from the following condition:

$$\nabla R_{\rm th}(D_{A_1}, D_{A_2}, \cdots, D_{A_N}) = 0 \tag{10}$$

where the operator ∇ represents the gradient of the scalar function $R_{\rm th}$ and N is the total number of layers between the active region and the heat sink.

Two problems arise from this formulation. If no restriction is made regarding the substrate diameter, one can find a device configuration that leads to the minimum thermal resistance achievable. When the substrate dimensions are given, the best thermal path in the laser structure is found. Both problems require the solution of a sparse system of nonlinear equations in the variables $D_{A_1}, D_{A_2}, \cdots, D_{A_N}$.

III. Unblocked Heat-Flux Propagation

The first situation to be considered is the case in which the heat flux propagates toward the heat sink with no restriction regarding the lateral dimensions of the chip. This approach is useful to determine the substrate diameter that leads to the minimal thermal resistance. Equation (10) represents a system of nonlinear equations for the variables $D_{A_i}, i = 1, 2, \cdots, N$. A top-emitting VCSEL, like the one studied here, may have more than 100 layers between the active region and the heat sink. In order to avoid the problem of finding a good initial guess for the solution of this large system of equations, we have adopted an iterative approach. It consists of fixing up, step by step, layers below the active region. In order to obtain an initial guess for the solution of the system of equations, it is assumed that an introduced layer practically unaffects the heat flux on the layers placed above it. Also, a complete spreading is expected to occur inside each added layer. Obviously, this approach is valid only if the introduced layer is thin enough, like the quarter-wave layers and the graded interfaces. In order to consider its effect on the heat-flux propagation, the substrate, which is much thicker than all others layers, must be subdivided in sub-layers to assure the convergence of the method.

In step L of the above-described procedure, one has to find the zero of a vector function $\vec{F}(D_{a_1}, D_{A_2}, \cdots, D_{A_L})$ whose components are given by

$$F_i = \frac{8d_i \cdot k_{r_{i+1}}}{\pi} + \frac{3k_{z_i} \cdot k_{r_{i+1}}}{4k_{r_i}} \cdot D_{A_i}^{1/2} \cdot (D_{A_i} - D_{A_{i-1}})^{1/2} - \frac{k_{z_i} \cdot D_{A_i}}{2} \cdot \left(1 - \frac{D_{A_i}}{D_{A_{i+1}}}\right)^{1/2} \left(1 + \frac{D_{A_i}}{2D_{A_{i+1}}}\right), \quad \text{for } i = 1, 2, \cdots, L-1 \tag{11}$$

$$F_L = -\frac{8d_L}{\pi} \cdot k_{r_L} + \frac{3}{4} \cdot k_{z_N} \cdot D_{A_N} \left(1 - \frac{D_{A_{n-1}}}{D_{A_N}}\right)^{1/2}. \tag{12}$$

During step L of the method, a good initial guess is obtained as follows:

$$D_{A_i}^{(L)} = D_{A_i}^{(L-1)}, \qquad \text{for } i = 1, 2, \cdots, L-1 \tag{13}$$

$$D_{A_L}^{(L)} = \frac{D_{A_{L-1}} + \sqrt{D_{A_{L-1}}^2 + \dfrac{4096 d_L^2 \cdot k_{r_L}^2}{9\pi^2 \cdot k_{z_L}^2}}}{2}. \tag{14}$$

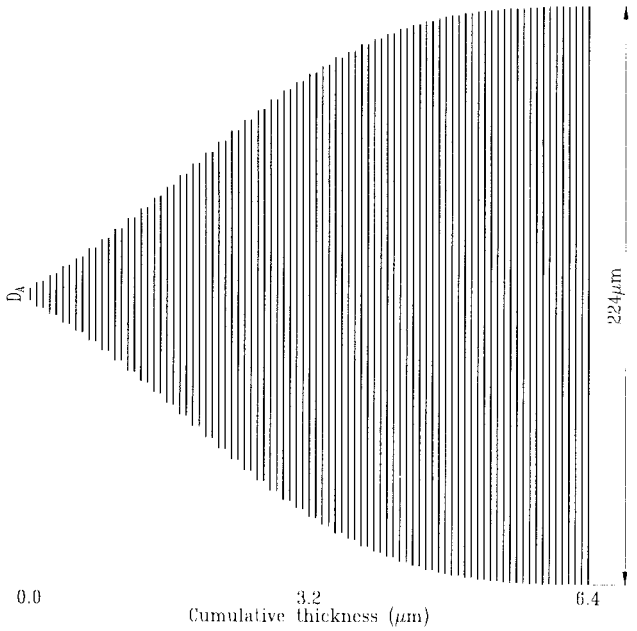

Fig. 2. 2-D heat-flux profile inside a PITSEL with 45.5 periods mirror at bottom DBR. The active-region diameter was 5 μm. The substrate thickness is close to zero and its effect was not considered.

The L-dimensional system in step L is solved by the Newtons method. The corresponding Jacobean matrix can be calculated in a closed form and is given by

$$J_{i,i} = \frac{3}{4} \cdot \frac{k_{z_i} \cdot k_{r_{i+1}}}{k_{r_i}} \cdot \left(1 - \frac{D_{A_{i-1}}}{2D_{a_i}}\right) \cdot \left(1 - \frac{D_{A_{i-1}}}{D_{A_i}}\right)^{1/2} - \frac{k_{z_i}}{2} \cdot \left(1 - \frac{D_{A_i}}{D_{A_{i+1}}}\right)^{-1/2} \cdot \left(1 - \frac{5}{4} \frac{D_{A_i}^2}{2D_{A_{i+1}}^2} - \frac{D_{A_i}}{2D_{A_{i+1}}}\right), \quad \text{for } i = 1, 2, \cdots, L-1 \tag{15}$$

$$J_{i,i+1} = -\frac{3}{8} \cdot k_{z_i} \cdot \left(\frac{D_{A_i}}{D_{A_{i+1}}}\right)^3 \cdot \left(1 - \frac{D_{A_i}}{D_{A_{i+1}}}\right)^{-1/2}, \quad \text{for } i = 1, 2, \cdots, L-1 \tag{16}$$

$$J_{i,i-1} = -\frac{3}{8} \cdot \frac{d_{z_i} \cdot k_{r_{i+1}}}{k_{r_i}} \cdot D_{A_i}^{1/2} \cdot (D_{A_i} - D_{A_{i-1}})^{-1/2}, \quad \text{for } i = 2, \cdots, L-1 \tag{17}$$

$$J_{L,L} = \frac{3}{4} \cdot k_{z_L} \cdot \left(1 - \frac{D_{A_{L-1}}}{2D_{A_L}}\right) \cdot \left(1 - \frac{D_{A_{L-1}}}{D_{A_L}}\right)^{-1/2} \tag{18}$$

$$J_{L,L-1} = -\frac{3}{8} \cdot k_{z_L} \cdot D_{A_L}^{1/2} \cdot \left(1 - \frac{D_{A_{L-1}}}{D_{A_L}}\right)^{-1/2}. \tag{19}$$

The Jacobean matrix, represented by (15)–(19) is tridiagonal. As a result, the computer memory requirement is greatly saved. Furthermore, this matrix is easily reduced to an equivalent triangular form.

Fig. 2 shows the 2-D heat-flux profile inside a typical PITSEL with a 45.5 period n-DBR mirror and a 5-μm active-region diameter. The effect of the substrate on which the structure is mounted was not considered. In Fig. 2, one can observe a step-like growing of the heat-flux propagation diameter, considering the thermal conductivity at room temperature

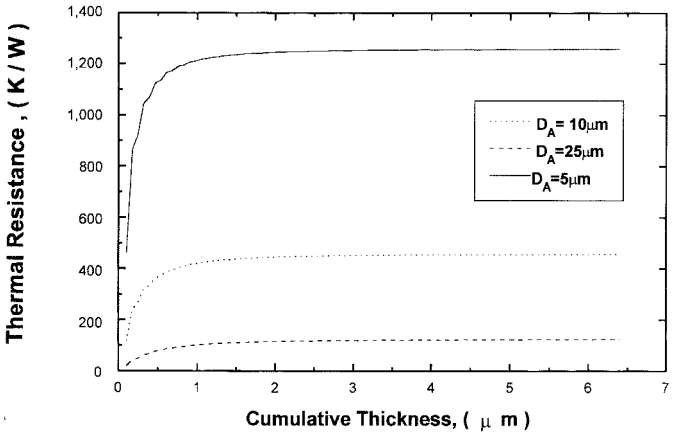

Fig. 3. Thermal resistance increasing with cumulative thickness of the DBR mirror. The PITSEL has 45.5 periods at bottom DBR. Three different active-region diameters were considered. The substrate thickness is close to zero and was not included in the calculations.

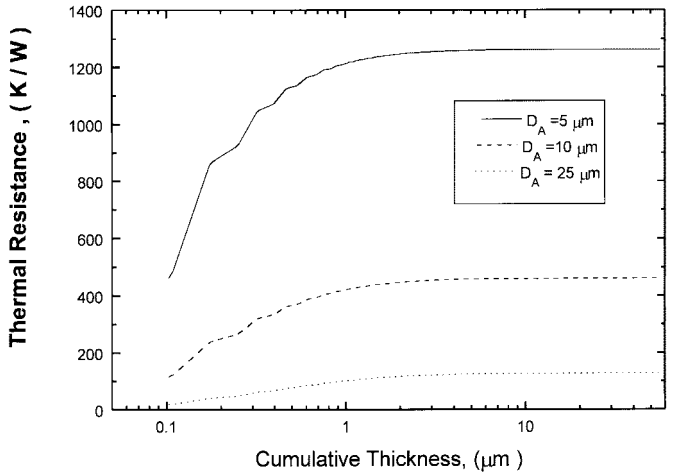

Fig. 4. Thermal resistance increasing with cumulative thickness in a PITSEL with 45.5 periods at bottom DBR for different active-region diameters. A 50-μm GaAs substrate was considered in calculations.

for the $Al_{0.15}Ga_{0.85}As$ equal to 16.87 W/m $\cdot$ K and for the AlAs equal to 91.67 W/m$\cdot$K. Quarter-wave layers of sensitive lateral scattering alternate with quarter-wave layers of closely vertical flux. At the low conductive $Al_{0.15}Ga_{0.85}$ layers, lateral spreading is small, while at the high conductive AlAs layers, scattering dominates.

Fig. 3 shows the thermal resistance as a function of the cumulative thickness of the DBR mirror for three different active-region diameters ($D_A = 5, 10$, and 25 μm). It can be concluded that the main contribution to the thermal resistance comes (in all cases illustrated) from the layers closer to the heat source (active region). In these layers, a strong lateral scattering is present. This spreading is more considerable in VCSEL's with small active regions, causing greater values of thermal resistance. It can also be seen in Fig. 3 that the thermal resistance increases while the lateral flux spread is incomplete, reaching a steady value at the remaining portion of the periodic structure.

Fig. 4 shows thermal resistance as a function of the cumulative thickness for the same PITSEL structure studied in Figs. 2 and 3. As before, the active-region diameters considered were 5, 10, and 25 μm. In this case, the presence of a 5-μm substrate is taken into account. Only a residual perturbation of the values shown in Fig. 3 can be seen. The introduction of a thick and uniform layer below the mirror grating causes a sensible alteration in the lateral spreading as to avoid a dramatic increase of the vertical thermal resistance. In order to illustrate this fact, a device with only 12.5 periods in the n-DBR is considered next. Fig. 5 shows the thermal resistance as a function of the cumulative thickness for a 50-μm PITSEL with a low reflective mirror. Two situations are represented there: with and without a 50-μm substrate placed below the mirror. Curves marked with $R_{\mathrm{th}_{V,B}}$ and $R_{\mathrm{th}_{S,B}}$ represent the thermal resistance components associated with vertical flux and lateral spreading, respectively, when no substrate is considered. Curves labeled with $R_{\mathrm{th}_{V,A}}$ and $R_{\mathrm{th}_{S,A}}$ represent the thermal resistance components associated with the vertical flux and lateral spreading, respectively, when the effect of the substrate is considered. We conclude that for this device the substrate increases the component associated with lateral scattering in 10%. Meanwhile, a simultaneous decrease of 6% is observed for the component associated to the vertical flux. As a consequence, the perturbation introduced by a 50-μm substrate over total thermal resistance value is less than 2%.

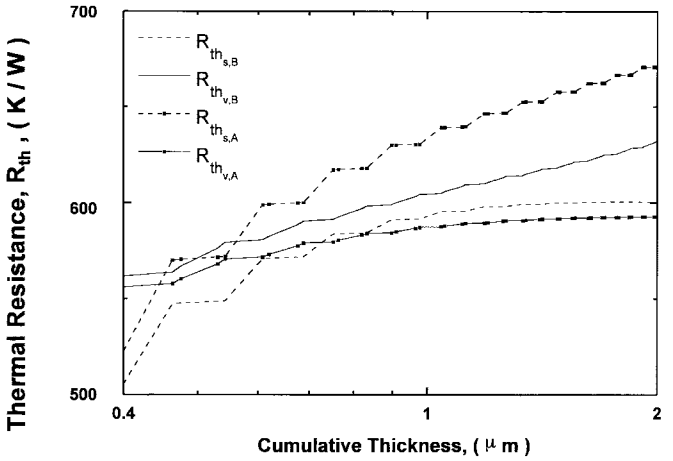

Fig. 5. Thermal resistance components associated to lateral spreading and vertical flux in a PITSEL with active-region diameter equal to 5 μm and 12.5 periods at n-DBR mirror.

Figs. 6 and 7 show, respectively, the 2-D heat-flux profile for a PITSEL with 12.5 n-DBR periods, when no substrate is placed below the mirror and when a 50-μm substrate is considered. Despite the small influence over the thermal resistance value, the substrate has a strong influence over the heat-flux profile and, therefore, over the temperature profile inside the chip.

As previously mentioned, in the process of finding the zeros of (11) and (12), the order of the system to be solved is incremented layer by layer from the active region down to the substrate, until the whole structure is considered. This method works well for all layers of the DBR grating. However, the inclusion of the substrate requires a little more attention since this medium is usually much thicker than all the others together and introduces a considerable perturbation in the

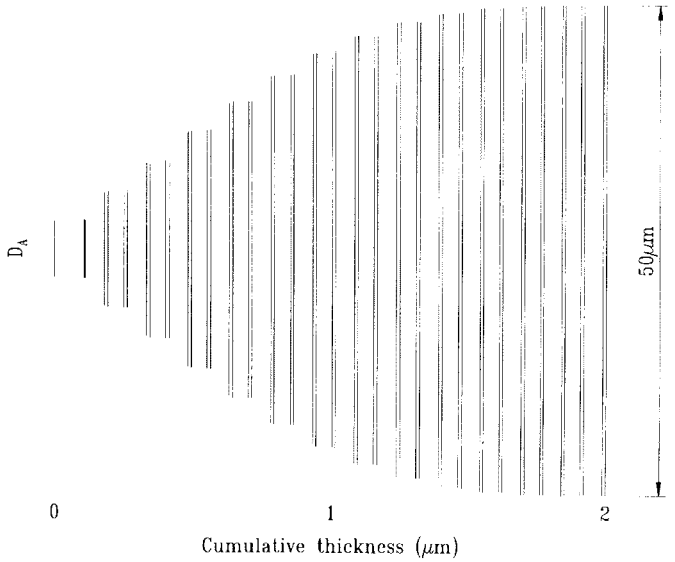

Fig. 6. 2-D heat-flux profile in a PITSEL with 5-μm active-region diameter and 12.5 periods at n-DBR. The effect of the substrate placed down the mirror was not considered at this point.

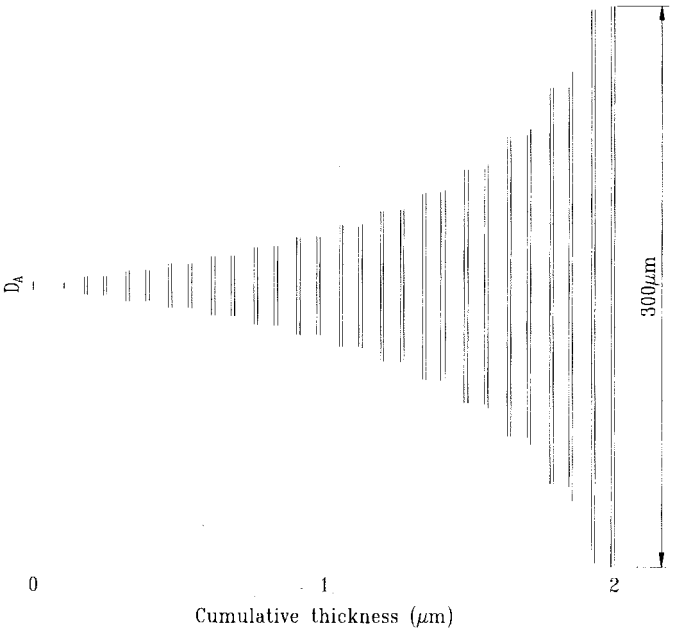

Fig. 7. 2-D heat-flux profile at n-DBR of a PITSEL with 5-μm active region and 12.5 periods in quarter-wave bottom mirror. The substrate diameter was 50 μm.

lateral spreading inside the chip. In order to skip the problem of obtaining an initial solution for the system of equations when the substrate is considered it was assumed that the substrate could be divided in several thinner layers. The heat-flux profile for the whole structure (including the substrate) is obtained by removing the thinner layers introduced inside the substrate. A comparison of the solutions achieved for the heat-flux profile with and without the above-mentioned subdivision is shown in Fig. 8. The output heat-flux diameter is shown in both situations for a PITSEL's with 45.5 period n-DBR mirror; the active-region diameter was varied from 5 to 100 μm. The dashed line shows the solution obtained when the substrate

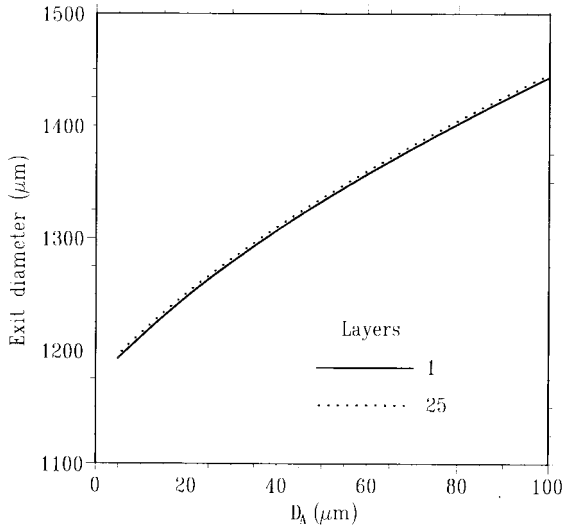

Fig. 8. Heat-flux exit diameter at substrate of a PITSEL with 45.5 periods at n-DBR, for different active-region diameters. Dotted line represents the solution obtained upon subdivision of substrate in 25 layers.

is divided in 25 sub-layers; the continuous line represents the solution obtained from refinement in the absence of the divisions. The difference between both solutions ranges from 0.2% to 0.4%, which is much less than the 2% error [10] obtained from the initial procedure approach given by (9).

IV. Blocked Heat-Flux Propagation

In this section, the previous approach is modified to allow the calculation of the thermal resistance of a VCSEL for a given substrate diameter. In this case, (10) must be rewritten as follows:

$$\frac{\partial R_{\text{th}}}{\partial D_{A_j}} = 0, \qquad \text{for } j = 1, 2, \cdots, N-1. \tag{20}$$

Equation (20) has the same structure as that of (10); however, it represents a system of a lower order. An iterative approach similar to that of the previous section will be used. During the first step, the nearest layer to the active region is introduced. In the following steps, the other layers are introduced underneath the previous ones; this procedure is repeated until the nearest layer to the substrate is considered. With this formulation, opposite to that of the earlier section, even the one-dimensional (1-D) problem will require a numerical solution, which can be obtained from a combination of bisection and Newton methods.

The vector function $\vec{F}(D_{A_1}, D_{A_2}, \cdots, D_{A_L})$ whose root has to be found during step L has the $(L-1)$ components described by (11). The highest order component is given by

$$F_L = -\frac{8d_L \cdot k_S}{\pi} + \frac{3k_{z_L} \cdot k_S}{4k_{r_L}} \cdot D_{A_L}^{1/2} \cdot (D_{A_L} - D_{A_{L-1}})^{1/2} - \frac{k_{z_L} \cdot D_{A_L}}{2} \cdot \left(1 - \frac{D_{A_L}}{D_S}\right)^{1/2} \left(1 + \frac{D_{A_L}}{2D_S}\right) = 0. \tag{21}$$

The Jacobean matrix of the system of equations mentioned above is formed by (15)–(17) and (19). The matrix highest

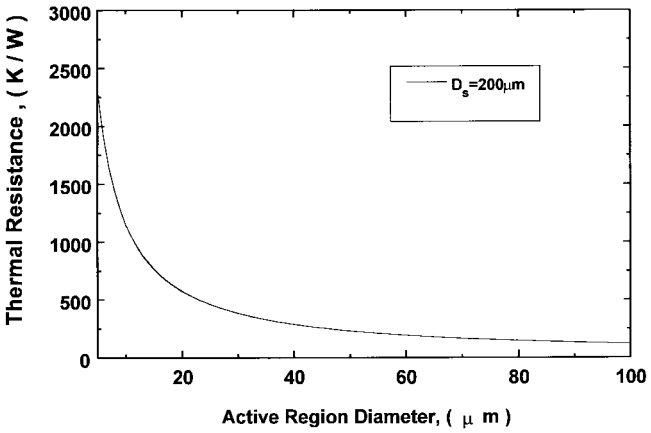

Fig. 9. Thermal resistance of a PITSEL with substrate diameter and thickness equal to 200 and 50 μm, respectively.

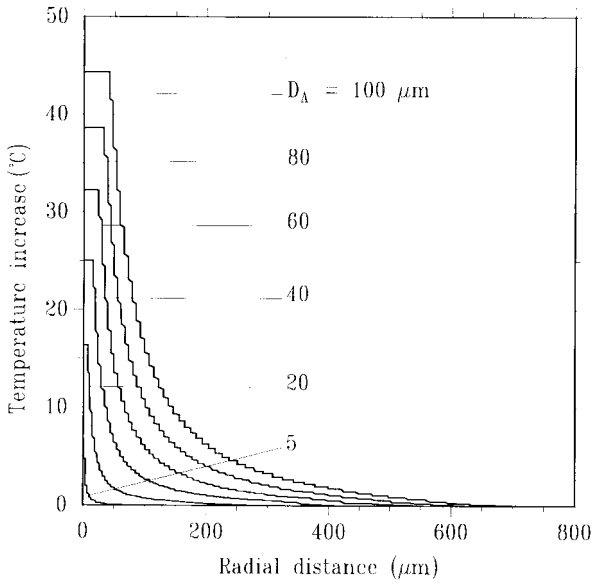

Fig. 10. Radial temperature profile inside a PITSEL for different active-region diameters.

order diagonal element is given by

$$J_{L,L} = \frac{3}{4}\,\frac{k_{z_L}\cdot k_S}{k_{r_L}}\cdot\left(1-\frac{D_{A_{L-1}}}{2D_{A_L}}\right)\left(1-\frac{D_{A_{L-1}}}{D_{A_L}}\right)^{-1/2} - \frac{k_{z_L}}{2}\cdot\left(1-\frac{D_{A_L}}{D_S}\right)^{1/2}\cdot\left(1-\frac{D_{A_L}}{2D_S}-\frac{5}{4}\,\frac{D_{A_L}^2}{D_S^2}\right). \tag{22}$$

In order to build an initial guess, the method of solution of this problem assumes, as for the case of the unblocked heat-flux propagation, that the influence of each introduced medium on the heat diffusion of the above layers is considerably weak.

Fig. 9 shows the thermal resistance of a typical laser configuration [7] as a function of the active-region diameter. The substrate diameter was considered to be 200 μm and the substrate thickness 50 μm. For a device with an active-region diameter 15 μm, we verified a good agreement between the experimental value [11] 800 K/W and the value 770 K/W observed in Fig. 9.

Based on the results described above for the heat-flux profile inside the laser chip, one can easily predict the radial temperature profile as follows:

$$\Delta T(r) = \sum_{i=1}^{N}\left[\int_0^{D_{A_i}/2} q\cdot(4\pi r)\cdot dr\right]\cdot R_{\mathrm{th}_i} \tag{23}$$

where $\Delta T(r)$ is the temperature as a function of the radial distance; q is the power thermal density $(\mathrm{W/cm^2})$ and R_{th_i} is thermal resistance component of the ith layer.

Considering the simplest case of a constant power thermal density inside the VCSEL ($q = 3$ kW/cm^2), the radial temperature profiles for different active-region diameters were obtained, as shown in Fig. 10. For a given power thermal density, the active-region temperature increases for wider active-region diameter. The long tail of the radial temperature profile shows the importance of employing small emitting units in order to avoid thermal cross-talk in 2-D arrays of PITSEL's.

V. Conclusion

The thermal resistance may become a key parameter to describe the thermal problems of VCSEL's. However, the methods that have used the thermal resistance approach to study the thermal influence over the VCSEL behavior are usually too simple and do not include multilayer aspects of heat propagation. In this paper, an approach to estimate the thermal resistance of a VCSEL where the heat-flux propagation is considered inside each one of the component layers of the device was presented. Two variations of this approach were considered. The first one is useful to determine the configuration that minimizes the active-region temperature, while the second one allows one to predict the thermal resistance of a given laser. From these results, the temperature profile inside the laser structure can be predicted once the heat power density is known. The results obtained here are useful for a simulation of the dynamic behavior of VCSEL's and for the calculation of the light-intensity/current (LI) curve.

References

[1] K. Iga, F. Koyama and S. Kinoshita, "Surface emitting lasers," *IEEE J. Quantum Electron.*, vol. 24, pp. 1845–1855, Sept. 1988.

[2] W. Ng, A. Walston, G. Tangonan, J. J. Lee, I. Newberg, and F. Bernstein, "The first demonstration of an optically steered microwave phased array," *J. Lightwave Technol.*, vol. 9, pp. 1124–1131, Sept. 1991.

[3] I. Frigyes, and A. J. Seeds, "Optically generated true-time in phased-array antennas," *IEEE Trans. Microwave Theory Tech.*, vol. 43, pp. 2378–2386, Sept. 1995.

[4] U. Fieldler, G. Reiner, P. Schnitzer, and K. J. Ebelin, "Top surface-emitting vertical-cavity laser diodes for 10-Gb/s data transmission," *IEEE Photon. Technol. Lett.*, vol. 8, pp. 746–748, June 1996.

[5] B. Tell, K. F. Brown-Goebeler, R. E. Leibenguth, F. M. Baez, and Y. H. Lee, "Temperature dependence of GaAs–AlGaAs vertical-cavity surface emitting lasers," *Appl. Phys. Lett.*, vol. 60, pp. 683–685, 1992.

[6] M. Osinski, W. Nakwaski, and A. Leal, "Effective thermal conductivity analysis of vertical-cavity top-surface-emitting lasers with semiconducting Bragg mirrors," in *Vertical-Cavity Surface-Emitting Laser Arrays*, J. L. Jewell, Ed., in *SPIE Int. Symp. Lasers, Sensors Applicat.*, Los Angeles, CA, Jan. 27–28, 1994, pp. 85–96.

[7] P. Zhou, J. Cheng, C . F. Schaus, S. Z. Sun, K. Zheng, E. Armour, C. Hains, W. Hsin, D. R. Myers, and G. A. Vawter, "Low series resistance high-efficiency GaAs/AlGaAs vertical-cavity surface-emitting lasers with continuously graded mirrors grown by MOCVD," *IEEE Photon. Technol. Lett.*, vol. 3, pp. 591–593, July 1991.

[8] W. Nakwaski, "Thermal conductivity of binary, ternary and quaternary III–V compounds," *J. Appl. Phys.*, vol. 64, pp. 159–166, 1988.
[9] S. Adachi, "GaAs, AlAs, and AlGaAs: Material parameters for use in research and device applications," *J. Appl. Phys.*, vol. 58, no. 3, pp. R1–R29, 1985.
[10] M. G. Cooper, B. B. Mikic, and M. M. Yovanovich, "Thermal contact conductance," *Int. J. Heat Mass Transf.*, vol. 12, pp. 279–300, 1969.
[11] C. C. Wu , K. Tai, and K. F. Huang, "Reliability studies of 0.85 μm vertical cavity surface emitting lasers: 50000h MTTF at 25 °C," *Electron. Lett.*, vol. 29, pp. 1953–1954, 1993.

Antonio A. Leal, photograph and biography not available at the time of publication.

Marek Osiński (SM'86) was born in Wroclaw, Poland, on May 28, 1948. He received the M.Sc. degree in theoretical physics from Warsaw University, Warsaw, Poland, in 1971, and the Ph.D. degree in physical sciences from the Institute of Physics of the Polish Academy of Sciences (PASc), Warsaw, Poland, in 1979.

In 1971, he joined the Institute of Physics, PASc, where he was engaged in investigations of wave-guiding properties and modal characteristics of semiconductor lasers. From 1980 to 1984, he was a Visiting Research Fellow at Southampton University, Southampton, U.K., where he conducted research on long-wavelength injection laser properties relevant to optical-fiber communications. He also investigated optical properties of III–V compounds and heterostructures, including quantum-well devices. From 1984 to 1985, he was a British Telecom Senior Research Associate in coherent optical communication at Cambridge University, Cambridge, U.K., where he was involved in studying picosecond modulation, gain-switched spectra, external-cavity coupling, and injection locking of diode lasers. Since 1985, he has been Associate Professor at the Center for High Technology Materials (CHTM), University of New Mexico, Albuquerque, NM, where he is also a Faculty Member in the Department of Electrical and Computer Engineering and the Department of Physics and Astronomy. His initial work at CHTM included high-power semiconductor laser arrays, spatially filtered external-cavity coupling, side-mode injection locking, and material properties of AlGaAs and InGaAsP alloys. From 1988 to 1989, he held the NTT Endowed Chair in Telecommunications as Visiting Professor at the Research Center for Advanced Science and Technology, University of Tokyo, Tokyo, Japan. Since January 1997, he has been a Visiting Professor at the Satellite Venture Business Laboratory, University of Tokushima, Tokushima, Japan, where he is engaged in research on group-III nitride materials and devices. He has authored or co-authored over 270 technical papers, and holds five patents. He has co-edited four books of SPIE conference proceedings on *Physics and Simulation of Optoelectronic Devices*. Since January 1992, he has served as the North American editor of *Progress in Quantum Electronics*. His current main research interests include short-wavelength optoelectronic devices in group-recombination and optical gain in wide-bandgap materials, failure analysis and degradation mechanisms, radiation effects on optoelectronic devices, surface-emitting lasers and 2-D arrays, thermal properties of semiconductor lasers, and new materials for mid-infrared lasers.

Dr. Oriński is a member of IEEE Lasers and Electro-Optics Society (LEOS), the Optical Society of America, the International Society for Optical Engineering (SPIE), and the Materials Research Society. He is listed in *American Men and Women of Science*, *Who's Who in Science and Engineering*, *Dictionary of International Biography*, *Men of Achievement*, *Who's Who in the World*, and *Polish American Who's Who*.

Evandro Conforti (S'81–M'83–SM'92) was born in São Jose, J. Rio Preto, São Paulo, Brazil, on August, 30, 1947. He received the B.Sc. degree in electronic engineering from the Technological Institute of Aeronautics (ITA), Sao Jose dos Campos, Brazil, in 1970, the M.Eng. degree from Federal University of Paraiba (UFPb), Campina Grande, Brazil, in 1972, the M.A.Sc. degree from University of Toronto, Toronto, Ont., Canada, in 1978, and the Ph.D. degree in electrical engineering from Unicamp, Campinas, Brazil, in 1983.

From 1972 to 1973, he was a Staff Member of the Microelectronics Laboratory, University of São Paulo (USP), where he worked in microwave strip-line circuits. From 1974 to 1980, he was an Assistant Professor at UFPb, where his major interest was on microwave waveguide devices and antennas. In 1981, he joined Unicamp, working as the Dean of the Faculty of Electrical and Computer Engineering (FEEC) (1984–1987) and currently as a Professor of electrical engineering. He has authored over 50 papers in Brazilian and international periodicals and conferences, has co-authored one book, and holds five patents. His current research interests include semiconductor lasers and optical amplifiers, optical switching, and optical phase-locked loops.